The Journal of Neuroscience, April 1991, 11(4): 1032–1039

Distribution of Ca^{2+} Channels on Frog Motor Nerve Terminals Revealed by Fluorescent ω-Conotoxin

M. W. Cohen,[1] O. T. Jones,[2] and K. J. Angelides[2]

[1]Department of Physiology, McGill University, Montreal, Quebec, Canada H3G 1Y6, and [2]Department of Physiology and Molecular Biophysics, Baylor College of Medicine, Houston, Texas 77032

Tetramethylrhodamine-conjugated ω-conotoxin was used as a fluorescent stain (Jones et al., 1989) to determine the spatial distribution of voltage-gated Ca^{2+} channels along frog motor nerve terminals. Like native ω-conotoxin, the fluorescent toxin blocked neuromuscular transmission irreversibly. The fluorescent staining was confined to the neuromuscular junction and consisted of a series of narrow bands (in face views) or dots (in side views) approximately 1 μm apart. This characteristic staining pattern was prevented by pretreatment with ω-conotoxin and by prior denervation for 5–7 d. Combined fluorescence and phase-contrast optics indicated that the stain was on the synaptic rather than the nonsynaptic side of the nerve terminal. The bands and dots of stain proved to be in spatial register with the postsynaptic junctional folds, as revealed by combined staining of ACh receptors. It is concluded that the voltage-gated Ca^{2+} channels on frog motor nerve terminals are concentrated at active zones. The findings are consistent with the suggestion (Heuser et al., 1974; Pumplin et al., 1981) that the large intramembranous particles seen at freeze-fractured active zones are voltage-gated Ca^{2+} channels.

At chemical synapses throughout the nervous system, the release of neurotransmitter during synaptic transmission is triggered by the entry of Ca^{2+} ions through voltage-gated Ca^{2+} channels (Katz, 1969; Augustine et al., 1987). These Ca^{2+} channels, which normally open in response to the arrival of the presynaptic action potential, are much more concentrated at presynaptic sites than elsewhere along axons (Katz and Miledi, 1969; Miledi and Parker, 1981; Stockbridge and Ross, 1984) and therefore can be considered a presynaptic specialization. However, their spatial distribution at chemical synapses has not yet been established. One possibility is that they are distributed uniformly throughout the plasma membrane of the presynaptic element. Alternatively, it may be that they are clustered only at certain sites along the presynaptic membrane. One suggestion is that they are localized preferentially at active zones, where exocytosis of neurotransmitter is believed to occur (Couteaux and Pecot-Dechavassine, 1970), and coincide with the dense arrays of large intramembranous particles that are seen there in freeze-fracture studies (Heuser et al., 1974; Pumplin et al., 1981).

Received Aug. 7, 1990; revised Nov. 13, 1990; accepted Nov. 19, 1990.

This work was supported by grants from MRC of Canada to M.W.C. and NIH to K.J.A. We thank D. McDonald and G. Hébert for photographic assistance.

Correspondence should be addressed to M. W. Cohen, Department of Physiology, McGill University, 3655 Drummond Street, Montreal, Quebec, Canada H3G 1Y6.

Copyright © 1991 Society for Neuroscience 0270-6474/91/111032-08$03.00/0

Recently, it was discovered that ω-conotoxin (ωCT) binds irreversibly to, and blocks, voltage-gated Ca^{2+} channels on frog motor nerve terminals and on many other neurons (Kerr and Yoshikami, 1984; Gray and Olivera, 1988). Moreover, the toxin can be made fluorescent by conjugation with tetramethylrhodamine succinimidyl ester and used as a specific stain to detect sites where the Ca^{2+} channels are present in sufficiently high density (Jones et al., 1989). In the present study, we have used tetramethylrhodamine-conjugated ωCT (RωCT) to determine the spatial distribution of voltage-gated Ca^{2+} channels on frog motor nerve terminals. The results indicate that these channels are concentrated at active zones.

A brief account of the findings has been reported previously (Cohen et al., 1990b).

Materials and Methods

Dissections. Sartorius muscles were obtained from frogs (*Xenopus laevis*) weighing 0.5–1.5 gm. The rationale for using such small frogs was to facilitate penetration of toxins and other agents to all neuromuscular junctions within the muscle. The frogs were anesthetized in tricaine methanesulfonate, and the sartorius muscles were isolated, usually with their sciatic nerve attached, so that neuromuscular transmission could be tested. The standard bathing solution consisted of 67% (vol/vol) L15 and 0.5% (vol/vol) dialyzed horse serum. The calcium and magnesium concentrations in this solution are approximately 0.8 mM and 1.2 mM, respectively. For some experiments, the calcium concentration was increased by 2 mM by addition of $CaCl_2$. Except where noted otherwise, all experimental procedures were carried out at room temperature (23–25°C).

In 2 experiments, a denervated sartorius muscle was compared with an innervated sartorius muscle from the same frog. Denervation was achieved by resecting the spinal–sciatic nerve shortly after its exit from the spinal cord, leaving a gap of approximately 2 mm between the cut ends. Fine silk thread was tied tightly around both the proximal nerve stump and the distal nerve stump near their cut ends. After 5–7 d, the frogs were reanesthetized, and their sartorius muscles, with sciatic nerve attached, were isolated. Examination of the site of resection under the dissecting microscope revealed no evidence of any nerve fiber outgrowth from the proximal stump.

Electrical stimulation. Neuromuscular transmission was tested by stimulating the sciatic nerve with single, brief (0.1 msec) shocks delivered through a pair of chlorided silver-wire electrodes. The contraction response was viewed under the dissecting microscope at a magnification of 20–40×. When sciatic nerve–sartorius muscle preparations were kept in our standard bathing solution and not exposed to any toxin, neuromuscular transmission persisted without apparent diminution for at least 14 hr.

Staining procedures. Tetramethylrhodamine-conjugated ω-conotoxin (RωCT) was prepared as described previously (Jones et al., 1989). It was used at a concentration of 0.2 μM in the bathing solution. Muscle preparations were bathed in it for 2–3 hr and then rinsed for 1–5 hr. In some experiments, they were exposed to fluorescein-conjugated α-bungarotoxin (FαBT) during part of the rinse period in order to stain their acetylcholine receptors (AChRs) as well (Anderson and Cohen, 1974).

They were then fixed with 4% (wt/vol) formaldehyde in 90 mM phosphate buffer (pH, 7.3) and stored in the refrigerator.

To test for the specificity of the RωCT staining, in some experiments 1 of the 2 muscle preparations from the same frog was first bathed for 1 hr in native ω-conotoxin (ωCT) at a concentration of 0.1–0.2 μM before being exposed to RωCT.

In the 2 experiments involving denervated muscle, after fixation for 1 hr in the refrigerator, 2 strips were removed from each muscle. One muscle strip was stained by immunofluorescence for a 65-kDa integral membrane protein associated with synaptic vesicles (Bixby and Reichardt, 1985; Cohen et al., 1987, 1990a), and the other was stained histochemically for cholinesterase (see Anderson and Cohen, 1974). The muscle strips were then returned to the fixative.

Microscopy. After 2 d or more in refrigerated fixative, the muscles were rinsed, teased into individual or small groups of muscle fibers in 70% (vol/vol) glycerol, and then mounted on glass slides in a solution consisting of 10 mg/ml *p*-phenylenediamine, 10 mM sodium carbonate, and 90% (vol/vol) glycerol. The slides were stored at −16°C until examined in the microscope.

The mounted muscle fibers were viewed and photographed through oil-immersion objectives (×63, NA 1.4 or ×100, NA 1.3). Incident-light fluorescence optics, for rhodamine or fluorescein, and transmitted-light phase-contrast optics were used separately as well as in combination with each other. When used in combination, the intensity of the phase-contrast illumination was reduced to a sufficiently low level so that both the phase-contrast and fluorescence images could be photographed simultaneously on the same frame. Photographs were taken with Tri X or Tmax 3200 Kodak film. Exposure times were 1–2 min for the RωCT fluorescence and only a few seconds for the FαBT fluorescence and the synaptic vesicle immunofluorescence.

Results

Biological potency

Treatment with ωCT, by blocking presynaptic voltage-gated Ca^{2+} channels in frog muscle, results in a failure of nerve impulses to trigger the release of ACh from the motor nerve terminals (Kerr and Yoshikami, 1984). Under these conditions, electrical stimulation of the nerve fails to evoke any contraction response in the muscle. In *Xenopus* sciatic nerve–sartorius muscle preparations, complete failure of neuromuscular transmission also occurred during exposure to RωCT but after a longer delay. When the tests were made in our standard bathing solution, ωCT (0.1–0.2 μM) blocked neuromuscular transmission completely within 15 min. However, after 15 min in RωCT (0.2 μM), there was no apparent change in the strength of neuromuscular transmission. Rather, some reduction was apparent by 30 min, and the failure was complete by 45 min. Likewise, when the calcium concentration of the bathing solution was increased by 2 mM in order to increase the safety factor for neuromuscular transmission, complete failure occurred within 40 min in ωCT but not until 1.5–2 hr in RωCT. The failure of neuromuscular transmission, whether induced by RωCT or by ωCT, persisted even after prolonged (up to 5 hr) rinsing with toxin-free solution. On the other hand, direct stimulation of the muscle continued to evoke strong contractions. Furthermore, in control preparations that were not exposed to toxin, neuromuscular transmission persisted without any apparent diminution for at least 14 hr. These findings indicate that RωCT behaves like ωCT but is less potent. They are consistent with previous findings that have demonstrated that RωCT is effective but less potent than ωCT in blocking voltage-gated Ca^{2+} channels on rat hippocampal neurons in culture (Jones et al., 1989). Other toxins such as α-bungarotoxin also exhibit a reduced potency but no apparent loss of specificity when conjugated with fluorophores such as tetramethylrhodamine isothiocyanate (Anderson and Cohen, 1974).

Staining pattern and specificity

Face views of the staining pattern obtained with RωCT are shown in Figures 1*A* and 2*A*. This characteristic staining pattern was confined exclusively to the neuromuscular junction, as revealed by combined staining of AChRs with FαBT (Fig. 1*A,B*). Like the FαBT fluorescence, the RωCT fluorescence consisted of a series of narrow bands, approximately 1 μm apart, oriented mainly perpendicularly to the long axis of the neuromuscular junction. However, the RωCT fluorescence was relatively faint and required photographic exposure times of 1–2 min, more than an order of magnitude greater than those for the FαBT fluorescence. Pretreatment with ωCT eliminated the characteristic banded pattern of RωCT fluorescence at the neuromuscular junction (Fig. 1*C,D*), thereby indicating that RωCT binds to the same sites as ωCT.

In addition to the characteristic banded appearance of the RωCT fluorescence, junctional and extrajunctional regions of the muscle fiber sometimes exhibited variable numbers of small bright patches, about 0.5–1.5 μm in diameter (Figs. 1*A*, 2*A*). These patches were not eliminated by pretreatment with ωCT (Fig. 1*C*), thereby indicating that they were not due to binding of RωCT to ωCT-sensitive Ca^{2+} channels. Because the occurrence of these nonspecific patches of fluorescence was highly variable, no further attempt was made to examine their basis. In muscles pretreated with ωCT, there was also a much fainter, diffuse fluorescence associated with some neuromuscular junctions (Fig. 1*C*). Background muscle fluorescence was also low and variable and was generally more apparent in larger-diameter muscle fibers.

In side views, the RωCT fluorescence consisted of a series of aligned dots occurring at intervals of approximately 1 μm (Figs. 2*B*, 3*A*). These dots were approximately 0.3 μm in diameter, corresponding in size to the width of the narrow bands seen in face views (cf. Fig. 2*A,B*). Also like the face-view bands, the side-view dots of RωCT fluorescence were confined entirely to the neuromuscular junction (Figs. 3–5) and were eliminated by pretreatment with ωCT.

The characteristic staining patterns seen in face and side views were observed even when RωCT-stained muscles were rinsed with toxin-free solution for up to 5 hr. This finding indicates that the specific binding of RωCT is essentially "irreversible," which is in agreement with our tests on neuromuscular transmission (see above). The staining patterns also indicate that the specific binding sites for RωCT have a highly nonuniform distribution along the length of the neuromuscular junction.

Effect of denervation

To check that the specific binding of RωCT was associated with the motor nerve terminals, muscles were examined after 5–7 d of denervation. It is known from the work of Birks et al. (1960b) that frog motor nerve terminals exhibit extensive degeneration after 5 d of denervation and can no longer function in synaptic transmission. This proved to be the case in the present study as well. Tests for neuromuscular transmission prior to treatment with toxin were negative even though direct stimulation of the denervated muscles elicited strong contractions. Second, immunofluorescent staining indicated that clusters of synaptic vesicles were present along the entire length of innervated neuromuscular junctions (Fig. 3*B*), whereas at denervated neuromuscular junctions they were rare or absent (Fig. 3*D*).

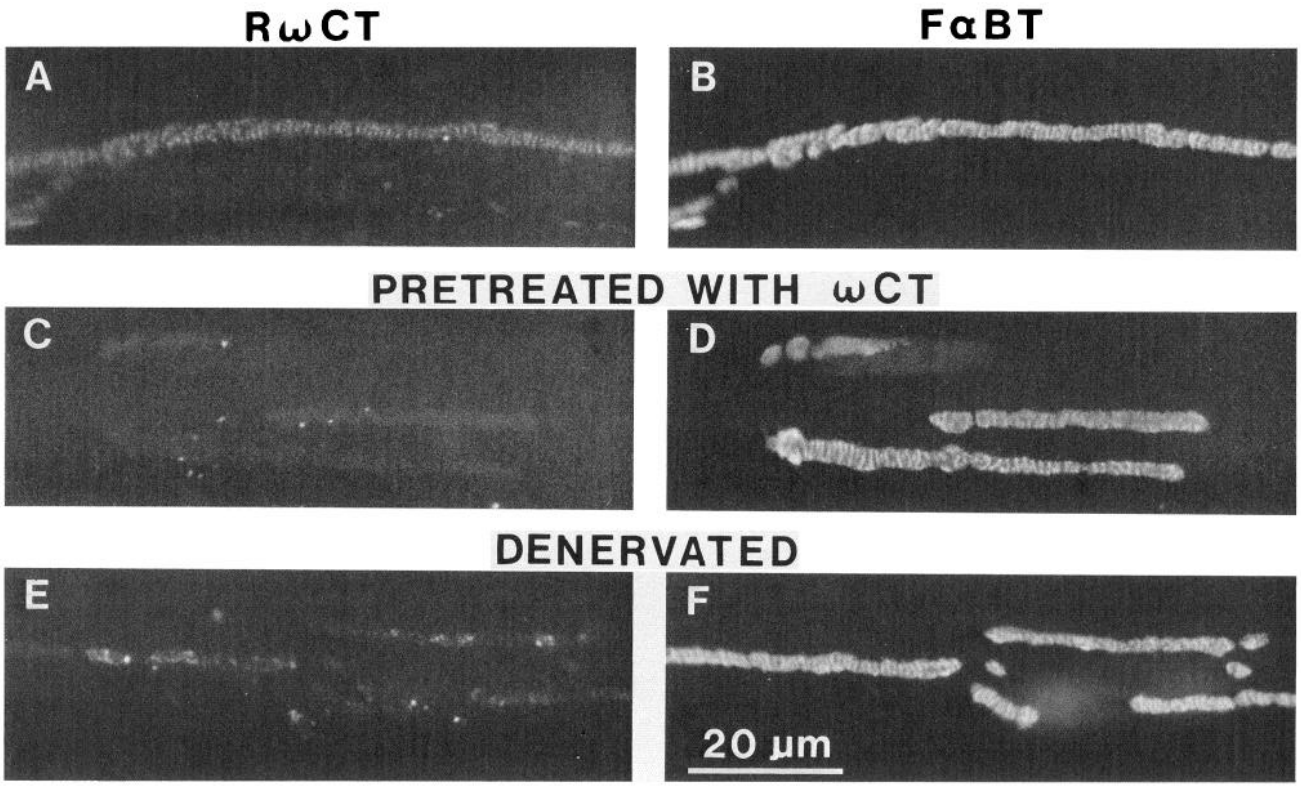

Figure 1. RωCT staining at the neuromuscular junction and its inhibition by pretreatment with ωCT and by denervation. Neuromuscular junctions were identified with fluorescein optics after staining AChRs with FαBT (*B, D, F*). The same junctions were also examined with rhodamine optics for RωCT fluorescence (*A, C, E*). *A* and *B,* Localization of RωCT at the neuromuscular junction. The RωCT fluorescence has a characteristic banded appearance (see also Fig. 2*A*), similar to the FαBT fluorescence, but is relatively faint. It is situated at the same site on the muscle cell as is the FαBT fluorescence. Also apparent in *A* is a small bright patch of fluorescence. *C* and *D* are from a muscle that was pretreated with ωCT before exposure to RωCT. The characteristic banded pattern of RωCT fluorescence seen in *A* is absent, but some small bright patches are apparent. *E* and *F* are from a muscle that was denervated for 5 d. The denervated neuromuscular junction exhibits very limited regions of RωCT fluorescence, whereas its FαBT fluorescence appears normal. Scale bar in *F* applies to *A–F.*

As indicated by the example of Figure 1*E,* even after 5 d of denervation the neuromuscular junctions exhibited very little of the characteristic RωCT fluorescence seen at control neuromuscular junctions. After 7 d of denervation, RωCT fluorescence was virtually absent (Fig. 3*C*). On the other hand, the denervated neuromuscular junctions were, as expected (see Anderson and Cohen, 1974), indistinguishable from control neuromuscular junctions with respect to FαBT staining of AChRs (Figs. 1*F,* 3*D*). Also in line with previous work (Letinsky et al., 1976), the pattern and intensity of cholinesterase staining appeared unaffected by these short periods of denervation. Considered together, the observations indicate that the characteristic RωCT fluorescence at innervated neuromuscular junctions was restricted to the motor nerve terminals. This is in line with the conclusion based on previous studies that, in frog muscle, ωCT binds selectively to the voltage-gated Ca^{2+} channels on the motor nerve terminals (Kerr and Yoshikami, 1984; Gray and Olivera, 1988).

Localization at active zones

To determine with more precision the spatial distribution of the RωCT-stained Ca^{2+} channels on the motor nerve terminals, we examined side views of the RωCT fluorescence and FαBT fluorescence with respect to their location on phase-contrast images of the neuromuscular junction. An example is illustrated in Figure 4. Figure 4*A* shows a phase-contrast view. The lower portion of the micrograph is occupied by a striated muscle fiber. At the edge of the muscle fiber, and extending approximately 1 μm above it, is a long nonstriated structure that consists of the motor nerve terminal and its thin overlying Schwann cell process (see Birks et al., 1960a). The boundary between the nerve terminal and the Schwann cell process cannot be resolved. In Figure 4*B,* the RωCT fluorescence is seen in combination with the phase-contrast image. It is apparent that the characteristic dots of RωCT fluorescence are situated at the boundary between the nerve terminal and the muscle cell, thereby indicating that the bound RωCT was on the synaptic rather than the nonsynaptic side of the motor nerve terminal. Further support for this interpretation is provided by Figure 4, *C* and *D.* Figure 4*C* shows the FαBT fluorescence in combination with the phase-contrast image. Because the FαBT fluorescence is associated with the AChRs on the postsynaptic membrane, it demarcates the boundary between the muscle fiber and the motor nerve terminal. Figure 4*D* is exactly the same as *C,* except that the position of the prominent dots of RωCT fluorescence has been denoted by small black squares. That they overlap the FαBT fluorescence confirms their location on the synaptic side of the motor nerve terminal.

Closer examination of Figure 4*C* reveals that the FαBT fluorescence consists of a narrow line with small dots extending downward toward the interior of the muscle cell (see also Figs. 3*D,* 5). These dots occur at intervals of approximately 1 μm

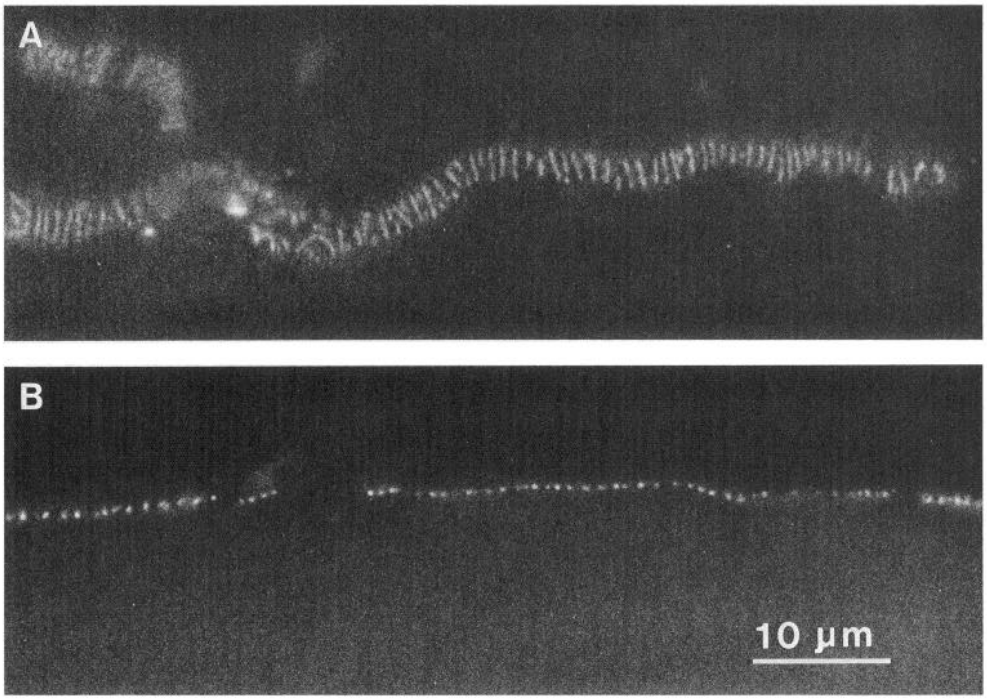

Figure 2. Nonuniform distribution of RωCT fluorescence at neuromuscular junctions. *A,* Face view, as in Figure 1. The RωCT fluorescence consists of a series of narrow bands, approximately 1 μm apart, oriented mainly perpendicular to the long axis of the neuromuscular junction. Also present are a couple of bright, nonspecific patches of fluorescence. *B,* Side view, showing RωCT fluorescence along part of a neuromuscular junction at the edge of a muscle cell. The fluorescence consists of a series of dots separated from each other by approximately 1 μm. The aligned dots that compose this characteristic staining pattern are smaller and fainter than the nonspecific patches of fluorescence seen in *A* (and in Fig. 1). Both *A* and *B* are from a muscle that was not exposed to FαBT. Scale bar in *B* also applies to *A*.

and arise because the high density of AChRs in the postsynaptic membrane extends partly into the junctional folds (Anderson and Cohen, 1974; Fertuck and Salpeter, 1974; Matthews-Bellinger and Salpeter, 1978). Accordingly, the small dots of FαBT fluorescence mark the sites of the junctional folds. It can be seen in Figure 4*D* that the dots of RωCT fluorescence are spatially aligned with the dots of FαBT fluorescence.

The precision of this alignment is seen more clearly in Figure 5, which is a montage of 2 photographs showing side views of the RωCT fluorescence (above) and the FαBT fluorescence (below) at the same neuromuscular junction. Virtually all the dots of RωCT fluorescence are aligned precisely with the dots of FαBT fluorescence. Similarly, in face views there was a high incidence of alignment between the narrow bands of RωCT fluorescence and the narrow bands of FαBT fluorescence (Fig. 6). The latter reflect the sites where the high density of AChRs in the postsynaptic membrane extends partly into the junctional folds (Anderson and Cohen, 1974). Altogether, the position of more than 1900 bands and dots of RωCT fluorescence at 29 neuromuscular junctions was compared to the position of the bands and dots of FαBT fluorescence and the incidence of alignment was 88% (Table 1). The 12% nonalignment may have been an experimental artifact arising from small changes in focus during the long (1–2 min) exposures needed to photograph the

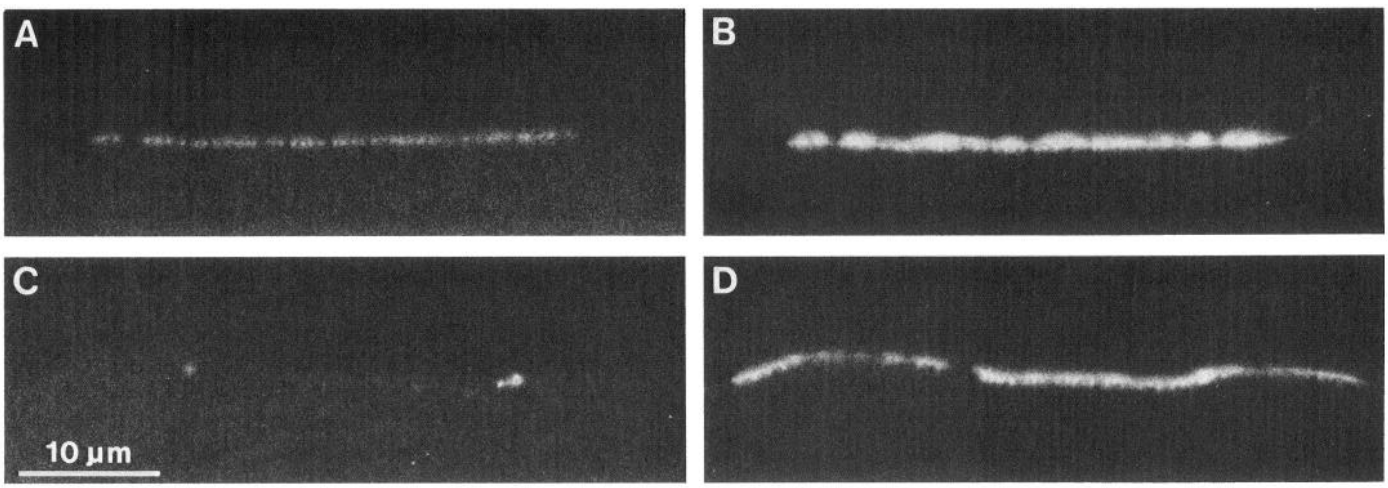

Figure 3. Side view of staining patterns at innervated (*A, B*) and 7-d-denervated (*C, D*) neuromuscular junctions. RωCT fluorescence is shown in *A* and *C,* and combined FαBT fluorescence and synaptic vesicle immunofluorescence is shown in *B* and *D*. At the denervated neuromuscular junction, only FαBT stain is seen (*D*). It consists of a narrow line with dots, approximately 1 μm apart, extending downward towards the interior of the muscle cell (see also Figs. 4*C,* 5). At the innervated neuromuscular junction, broad patches of synaptic vesicle immunofluorescence lie on the FαBT fluorescence and extend approximately 1 μm above it (*B*). Characteristic dots of RωCT fluorescence are seen at the innervated (*A*) but not at the denervated (*C*) neuromuscular junction. Scale bar in *C* applies to *A–D*.

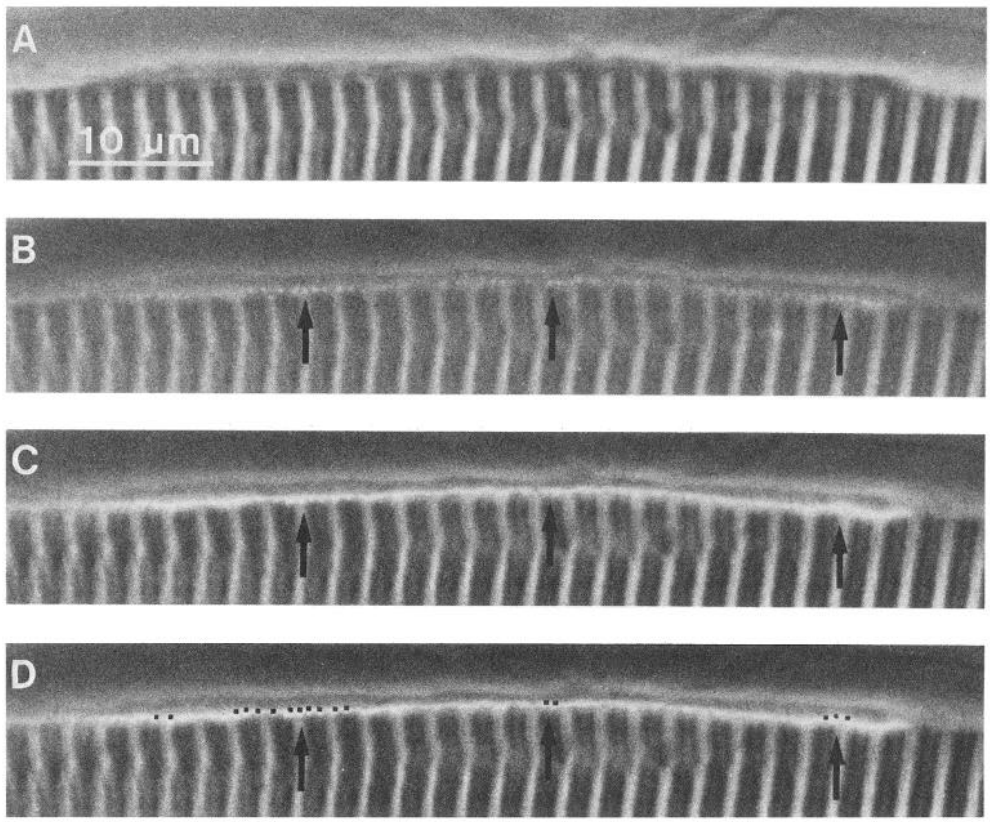

Figure 4. Localization of RωCT fluorescence on the synaptic side of the motor nerve terminal. *A,* Phase-contrast view of part of a muscle cell. The nonstriated structure associated with the edge of the muscle cell includes the motor nerve terminal and its overlying Schwann cell process. *B,* Phase-contrast image combined with RωCT fluorescence. Characteristic, aligned dots of RωCT fluorescence (*arrows*) delineate the region of apposition between the motor nerve terminal (*above*) and the striated muscle cell (*below*). *C,* Phase-contrast image combined with FαBT fluorescence. The FαBT fluorescence marks the boundary between the nerve terminal and the muscle cell. Note that the FαBT fluorescence appears as a continuous line, and in some regions, characteristic dots of fluorescence can be seen extending slightly below the line (e.g., at *leftmost arrow*). *Arrows* have the same position as in *B. D,* Same as *C,* except that the position of the prominent dots of RωCT fluorescence is indicated by *solid squares.* The overlap between the RωCT fluorescence and the FαBT fluorescence indicates that the former must be associated with the synaptic rather than the nonsynaptic side of the motor nerve terminal. Also apparent in some regions (e.g., at *leftmost arrow*) is that the dots of RωCT fluorescence are aligned with the dots of FαBT fluorescence.

RωCT fluorescence. In any event, it is apparent from the present results that most, if not all, of the presynaptic clusters of Ca^{2+} channels face the junctional folds. Presynaptic sites that face junctional folds exhibit unique ultrastructural specializations and are referred to as active zones because they are believed to be the main sites of exocytosis (Birks et al., 1960a; Couteaux and Pecot-Dechavassine, 1970; Heuser et al., 1974).

In side views, the intensity of neighboring dots of RωCT fluorescence varied considerably (Figs. 2*B,* 5), whereas in face views, the neighboring bands of RωCT fluorescence exhibited more closely matched intensities (Figs. 2*A,* 6). The greater variability in side views presumably arises from the fact that some active zones are shorter than their neighbors and some are not oriented perpendicularly to the long axis of the nerve terminal (Figs. 1*A,* 2*A,* 6). In side views, the RωCT fluorescence at the shorter or angled active zones would appear less intense than at the longer, perpendicular ones. Furthermore, slight differences in the position of the active zones with respect to the plane of focus would also affect the intensity of the bands of RωCT fluorescence seen in face views. Based on these considerations, the results are consistent with the notion that neighboring active zones contain approximately similar densities of Ca^{2+} channels.

Table 1. Alignment between RωCT and FαBT fluorescence

Neuromuscular junctions	29
Bands and dots of RωCT fluorescence	1914
Number aligned with FαBT bands and dots	1692
Alignment	88.4%

As indicated by the arrows in Figures 5 and 6, only a small percentage of the junctional folds were not apposed by dots or bands of RωCT fluorescence. The apparent absence of RωCT fluorescence opposite these few junctional folds may be artifactual, in line with the considerations discussed above. Alternatively, it is known that at frog neuromuscular junctions the Schwann cell extends fine processes that interdigitate between the nerve terminal and the muscle fiber. At sites where these interdigitations face junctional folds, the nerve terminal lacks the ultrastructural features of active zones (Birks et al., 1960a). It may be that the junctional folds that were not apposed by RωCT stain were those where the nerve terminal lacked an active zone and had instead an interposing Schwann cell process between it and the junctional fold. Taken together, our results lead to the conclusion that voltage-dependent Ca^{2+} channels on frog motor nerve terminals are clustered only at active zones.

Discussion

In the present study, RωCT was used to assess how voltage-gated Ca^{2+} channels are distributed on frog motor nerve terminals. In agreement with previous work, we found that this fluorescent conjugate of ωCT is biologically active, though less potent than the native toxin (Jones et al., 1989), that it binds to the same sites as the native toxin (Jones et al., 1989), and that its binding, like that of the native toxin (Kerr and Yoshikami, 1984), is irreversible at the frog neuromuscular junction. As far as we know, ωCT binds selectively only to Ca^{2+} channels, and it is only by blocking these channels on motor nerve terminals that it eliminates neuromuscular transmission irreversibly (Kerr and Yoshikami, 1984; Gray and Olivera, 1988). That

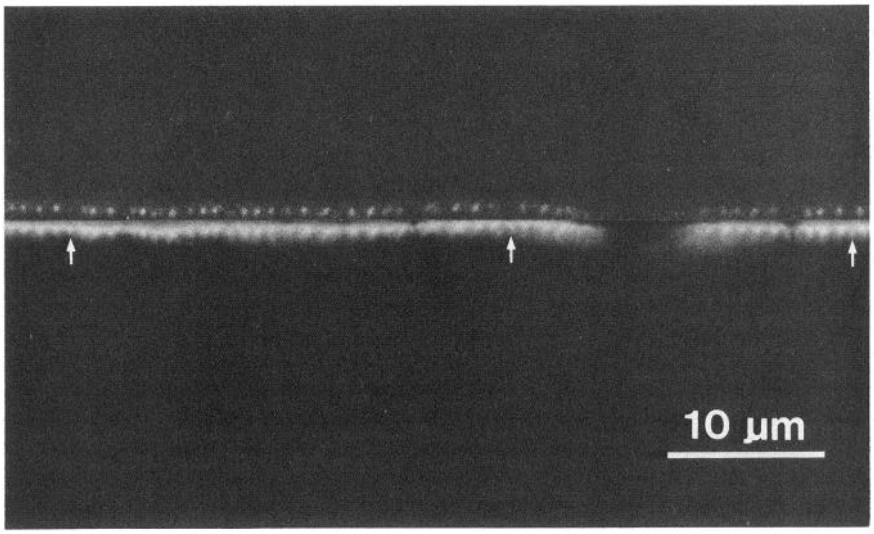

Figure 5. Photographic composite illustrating alignment between side views of RωCT fluorescence (*above*) and FαBT fluorescence (*below*). Virtually all dots of RωCT fluorescence occur in register with the dots of FαBT fluorescence. *Arrows* point to dots of FαBT fluorescence that are not associated with corresponding dots of RωCT fluorescence.

the ωCT binding was presynaptic is further supported by the finding that the binding sites were eliminated within 5–7 d following denervation. Previous studies have indicated that, at the frog neuromuscular junction, denervation leads to degeneration of the motor nerve terminals within 5 d but does not affect the survival of components of the synaptic basal lamina and of the postsynaptic membrane until much later (Birks et al., 1960b; Miledi, 1960; Letinsky et al., 1976; McMahan et al., 1980). In agreement with these previous studies, we observed no apparent changes in the staining pattern of AChRs or of cholinesterase at neuromuscular junctions that were denervated for 5–7 d. When considered together with our finding that the RωCT binding sites are directly apposed to the junctional folds, it follows that the calcium channels on frog motor nerve terminals are clustered at active zones. To make the alternative assumption that the RωCT fluorescence reflects the distribution of a synaptic component other than presynaptic Ca^{2+} channels, it would be necessary to postulate that both RωCT and ωCT bind irreversibly not only to the Ca^{2+} channels, but also to this additional synaptic component, and that the latter component is concentrated just outside the junctional folds, disappears rapidly after denervation, and is packed more densely than the Ca^{2+} channels. Although we have no way of excluding the existence of such a unique, as yet undiscovered, synaptic component, it seems much more reasonable to conclude instead that RωCT and ωCT bind selectively only to voltage-gated Ca^{2+} channels, and that the RωCT fluorescence reflects the distribution of these channels on frog motor nerve terminals.

Based on this conclusion, at least 2 different arrangements can be suggested for the spatial organization of Ca^{2+} channels at active zones. One possibility is that there is a single cluster of Ca^{2+} channels at each active zone (Fig. 7*A*). This arrangement is consistent with the observation that there was only a single band (in face views) or dot (in side views) of RωCT fluorescence in register with each junctional fold. Of course, even if the band of Ca^{2+} channels was only 100 nm wide (the same width as the junctional folds), the fluorescence originating from it after treatment with RωCT would appear somewhat wider (approximately 300 nm in the present study) because of light scattering. An alternative possibility, and the one we favor, is that the Ca^{2+}

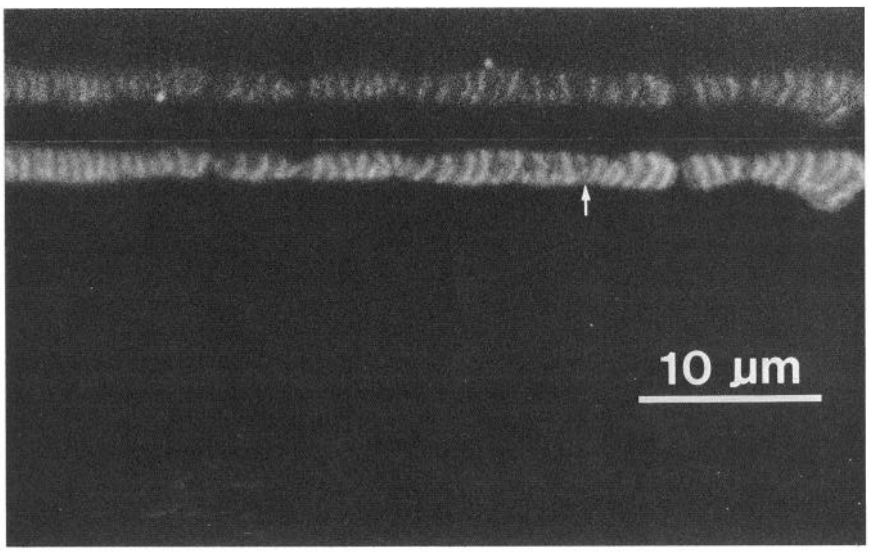

Figure 6. Photographic composite illustrating alignment between face views of RωCT fluorescence (*above*) and FαBT fluorescence (*below*). Virtually all bands of RωCT fluorescence are aligned with the bands of FαBT fluorescence. The *arrow* points to a band of FαBT fluorescence that is not associated with a corresponding band of RωCT fluorescence.

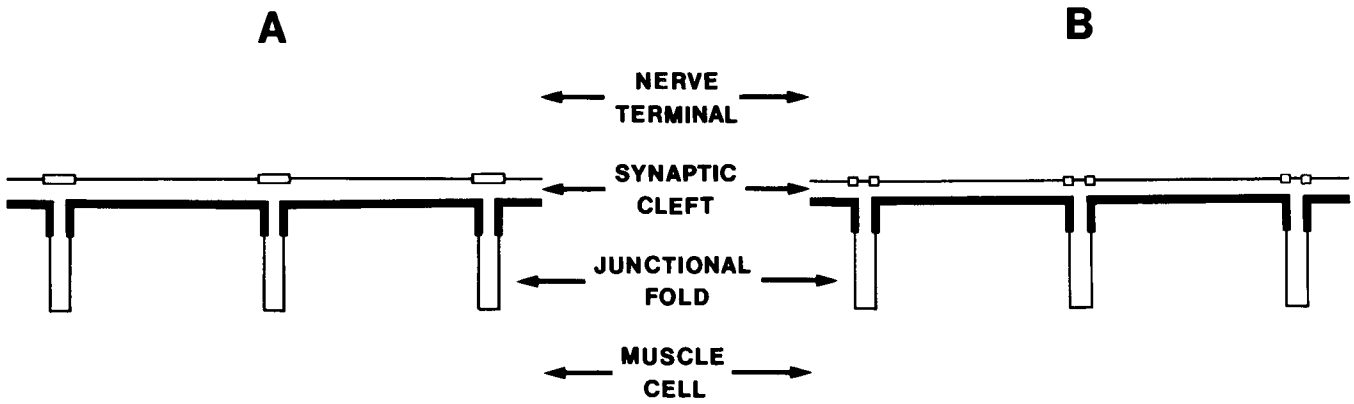

Figure 7. Alternative schemes for the distribution of presynaptic Ca^{2+} channels. *Open rectangles* indicate sites along the presynaptic membrane where Ca^{2+} channels are present in high density. *Thick solid lines* indicate sites along the postsynaptic membrane where AChRs are present in high density. Previous studies (see Results) have indicated that AChRs are present in high density throughout the postsynaptic membrane except in the deeper portions of the junctional folds. The present study indicates that presynaptic Ca^{2+} channels are clustered only at active zones, opposite the junctional folds. The results are consistent with a single cluster of Ca^{2+} channels extending the full width of each junctional fold (*A*) or 2 clusters, separated by 100 nm, in register with the sides of each junctional fold (*B*). A gap of 100 nm between 2 sources of fluorescent stain would not be resolved by fluorescence microscopy. Based on previous freeze-fracture studies (see Discussion), the arrangement in *B* seems more likely than that in *A*.

channels at each active zone are organized into 2 separate clusters (Fig. 7*B*). If these clusters were aligned with the walls of the junctional fold and separated from each other by only 100 nm, the gap between them would not be resolved by RωCT staining. Rather, it would be masked by the scattered fluorescence emanating from each cluster. In the same vein, the fluorescence originating from FαBT-stained AChRs does not reveal the gap at junctional folds (e.g., Figs. 5, 6). This arrangement of 2 narrow clusters at each active zone along frog motor nerve terminals is in agreement with the suggestion that the large intramembranous particles at active zones are voltage-gated Ca^{2+} channels (Heuser et al., 1974; Pumplin et al., 1981).

That Ca^{2+} channels are concentrated at active zones has obvious implications for synaptic transmission. For example, the elegant experiments of Katz and Miledi (1965) revealed that, at the frog neuromuscular junction, the synaptic delay of approximately 0.5 msec at 20°C is due mainly to a delay between the arrival of the presynaptic action potential and the release of neurotransmitter. This 0.5-msec delay can have several components: a delay in the opening of the Ca^{2+} channels, the time for the entering Ca^{2+} ions to diffuse to their intraterminal receptors, and the duration of the subsequent unknown reactions culminating in neurotransmitter release. The intraterminal receptors to which Ca^{2+} ions bind have not yet been identified, but it is widely believed that they are localized in the immediate vicinity of the active zone (Augustine et al., 1987). If this is the case, then the concentration of Ca^{2+} channels at active zones is an effective arrangement for achieving efficient triggering of neurotransmitter release. The very small diffusion distance would ensure that the entering Ca^{2+} ions achieve their highest concentration in the vicinity of their intraterminal receptors, and with minimal delay.

In our highest resolution micrographs (e.g., Figs. 2, 5), the RωCT fluorescence appeared to be restricted entirely to the active zones. If voltage-gated Ca^{2+} channels on frog motor nerve terminals are also present outside active zones, then their density there is too low to be reliably detected by the methods employed in the present study. A sharp decline in density beyond the active zones implies that there must be some anchoring mechanisms that prevent the Ca^{2+} channels from diffusing away from the active zones. Several related questions arise: Do the presynaptic Ca^{2+} channels share common anchoring mechanisms with the postsynaptic AChRs that are known to be immobile (Stya and Axelrod, 1984)? What accounts for their alignment with the junctional folds? At what point during neuromuscular synaptogenesis do these clusters of Ca^{2+} channels form? For the case of AChRs, it is known that, during synaptogenesis, preexisting mobile AChRs in neighboring extrajunctional regions accumulate, and become immobilized, at the site of nerve–muscle contact, thereby contributing to the buildup of the high-density of AChRs in the newly forming postsynaptic membrane (Anderson and Cohen, 1977; Ziskind-Conhaim et al., 1984; Kidokoro et al., 1986). Do similar mechanisms contribute to the accumulation of Ca^{2+} channels at developing active zones? In this regard, it is interesting to note that, in cultures of rat hippocampal neurons, a significant fraction of extrajunctional Ca^{2+} channels are mobile, whereas those that are clustered at synaptic sites are immobile (Jones et al., 1989). Just as the use of fluorescent and radioactive conjugates of α-bungarotoxin have proven so valuable in probing developmental changes in the number, distribution, and turnover of AChRs, so too the use of fluorescent and radioactive conjugates of ωCT may prove valuable in determining developmental changes in the number, distribution, and turnover of voltage-gated Ca^{2+} channels.

References

Anderson MJ, Cohen MW (1974) Fluorescent staining of acetylcholine receptors in vertebrate skeletal muscle. J Physiol (Lond) 237:385–400.

Anderson MJ, Cohen MW (1977) Nerve-induced and spontaneous redistribution of acetylcholine receptors on cultured muscle cells. J Physiol (Lond) 268:757–773.

Augustine GJ, Charlton MP, Smith SS (1987) Calcium action in synaptic transmitter release. Annu Rev Neurosci 10:633–693.

Birks R, Huxley HE, Katz B (1960a) The fine structure of the neuromuscular junction of the frog. J Physiol (Lond) 150:134–144.

Birks R, Katz B, Miledi R (1960b) Physiological and structural changes at the amphibian neuromuscular junction, in the course of nerve degeneration. J Physiol (Lond) 150:145–168.

Bixby JL, Reichardt LF (1985) The expression and localization of synaptic vesicle antigens at neuromuscular junctions *in vitro*. J Neurosci 5:3070–3080.

Cohen MW, Rodriguez-Marin E, Wilson EM (1987) Distribution of

synaptic specializations along isolated motor units in *Xenopus* nerve-muscle cultures. J Neurosci 7:2849–2861.

Cohen MW, Frair PF, Cantin C, Hébert G (1990a) Developmental changes in the half-life of acetylcholine receptors in the myotomal muscle of *Xenopus laevis*. J Physiol (Lond) 426:281–296.

Cohen MW, Jones OT, Angelides KJ (1990b) Distribution of calcium channels along frog motor nerve terminals. Soc Neurosci Abstr 16: 1274.

Couteaux R, Pecot-Dechavassine M (1970) Vesicules synaptiques et poches au niveau des "zones actives" de la jonction neuromusculaire. CR Acad Sci (Paris) 271:2346–2349.

Fertuck HC, Salpeter MM (1974) Localization of acetylcholine receptor by ^{125}I-α-bungarotoxin at mouse motor endplates. Proc Natl Acad Sci USA 71:1376–1378.

Gray WR, Olivera BM (1988) Peptide toxins from venomous *Conus* snails. Annu Rev Biochem 57:665–700.

Heuser JE, Reese TS, Landis DMD (1974) Functional changes in frog neuromuscular junctions studied with freeze-fracture. J Neurocytol 3:109–131.

Jones OT, Kunze DL, Angelides KJ (1989) Localization and mobility of ω-conotoxin-sensitive Ca^{2+} channels in hippocampal CA1 neurons. Science 244:1189–1193.

Katz B (1969) The release of neural transmitter substances. Liverpool: Liverpool UP.

Katz B, Miledi R (1965) The measurement of synaptic delay, and the time course of acetylcholine release at the neuromuscular junction. Proc R Soc Lond [Biol] 161:483–495.

Katz B, Miledi R (1969) Tetrodotoxin-resistant electrical activity in presynaptic terminals. J Physiol (Lond) 203:459–487.

Kerr LM, Yoshikami D (1984) A venom peptide with a novel presynaptic blocking action. Nature 308:282–284.

Kidokoro Y, Brass B, Kuromi H (1986) Concanavalin A prevents acetylcholine receptor redistribution in *Xenopus* nerve-muscle cultures. J Neurosci 6:1941–1951.

Letinsky MS, Fischbeck KH, McMahan UJ (1976) Precision of reinnervation of original postsynaptic sites in frog muscle after nerve crush. J Neurocytol 5:691–718.

Matthews-Bellinger J, Salpeter MM (1978) Distribution of acetylcholine receptors at frog neuromuscular junctions with a discussion of some physiological implications. J Physiol (Lond) 279:197–213.

McMahan UJ, Edgington DR, Kuffler DP (1980) Factors that influence regeneration of the neuromuscular junction. J Exp Biol 89:31–42.

Miledi R (1960) Acetylcholine sensitivity of frog muscle fibres after complete or partial denervation. J Physiol (Lond) 151:1–23.

Miledi R, Parker I (1981) Calcium transients recorded with arsenazo III in the presynaptic terminal of the squid giant synapse. Proc R Soc Lond [Biol] 212:197–211.

Pumplin DW, Reese TS, Llinas R (1981) Are the presynaptic membrane particles the calcium channels? Proc Natl Acad Sci USA 78: 7210–7213.

Stockbridge N, Ross WN (1984) Localized Ca^{2+} and calcium-activated potassium conductances in terminals of a barnacle photoreceptor. Nature 309:266–268.

Stya M, Axelrod D (1984) Mobility of extrajunctional acetylcholine receptors on denervated adult muscle fibers. J Neurosci 4:70–74.

Ziskind-Conhaim L, Geffen I, Hall ZW (1984) Redistribution of acetylcholine receptors on developing rat myotubes. J Neurosci 4:2346–2349.